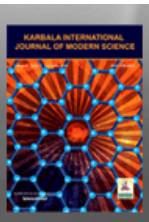

Karbala International Journal of Modern Science

Volume 12 | Issue 2 Article 4

Eco-assisted Ultrasonic Synthesis, Characterization, and Electrical Conductivity Study of Polyaniline/ Silica@Fe3O4 Q1 Nanocomposites

Ali Salim Shaway
Department of Chemistry, College of Science, Wasit University, Wasit, Kut, Iraq.

Kholoud Dham Khamkheem
Department of Physics, College of Science, University of Wasit, Kut, Iraq

Jawad Kadhim Abaies
Department of Chemistry, College of Science, Wasit University, Wasit, Kut, Iraq

Athra G. Sager
Department of Chemistry, College of Science, Wasit University, Wasit, Kut, Iraq, asaker@uowasit.edu.iq

Recommended Citation

Shaway, Ali Salim; Khamkheem, Kholoud Dham; Abaies, Jawad Kadhim; and Sager, Athra G. (2026) "Eco-assisted Ultrasonic Synthesis, Characterization, and Electrical Conductivity Study of Polyaniline/ Silica@Fe3O4 Q1 Nanocomposites," *Karbala International Journal of Modern Science*: Vol. 12 : Iss. 2 , Article 4.
Available at: https://doi.org/10.33640/2405-609X.3456

Eco-assisted Ultrasonic Synthesis, Characterization, and Electrical Conductivity Study of Polyaniline/ Silica@Fe3O4 Q1 Nanocomposites

Abstract

ومركبات نانوية قائمة على البولي أنيلين (Fe_3O_4) وفي هذه الدراسة الصوتية، أصبحت السيليكا المُنتجة بأكسيد الحديد (Fe_3O_4) مُطعّم بنسبة 5-15% من السيليكا المُعزز للحديد. وأكملت نهائيا ماء أنيلين والمركبات العلمية المتنوعة. أن حجم جسيمات البولينج أنيلين XRD وأحدثت نتائج TEM.وSEM وXRDو UV-Visو FT-IR الارتباط باستخدام تقنيات الناي (PANI) يبلغ 55.5. مكثف هذا الحجم إلى 45.2 عند تطعيم بولي أنيلين بنسبة 15% وزناً من السيليكا المُغلفة بأكسيد الحديد (Fe_3O_4) مُحضّرة بطريقة جيدة بشكل جيد، مما يميل إلى التمدد بشكل ثابت في تشكيل المركب المتباين المنظم. ضاقت النطاق البصري من 3.2 إلى 2.5 إلكترون فولت مع زيادة نسبة المطعّم، مما يشير إلى تفاعلي المُطعّم غير PANI المتوقع الشحنة. علاوة على ذلك، لا سيء من الملحوظ بشكل ملحوظ إلى الموصلية الكهربائية لـ PANI الصوتي لـ كما وُجِد أن الموصلية الكهربائية للعيادة نسبة ذات زيادة في وزن التطعيم فقط بسبب الحرارة. ولهذا السبب فإن هذه النتائج هي أن السيليكا المُصنعة بطريقة صديقة للبيئة والمُغطية بأكسيد الحديد الثلاثي (Fe_3O_4) تُحسّن PANI، بشكل أفضل إختيار الإيديوي والكهربائي لـ مما يُسلط الضوء على التعاون الجديد إنتاج موصل متعدد الفرق متميز لـ واعدة إلكترونية.

Keywords

Conductivity; Green chemistry; Magnetite; Nanoparticle; polyaniline; Silica.

Cover Page Footnote

Acknowledgment The authors would like to thank the College of Science, University of Wasit, for providing the necessary facilities.

RESEARCH PAPER

Eco-assisted Ultrasonic Synthesis, Characterization, and Electrical Conductivity Study of Polyaniline/ Silica@Fe_3O_4 Nanocomposites

Ali S. Shaway [a], Kholoud D. Khamkheem [b], Jawad K. Abaies [a], Athra G. Sager [a,*]

[a] Department of Chemistry, College of Science, Wasit University, Wasit, Kut, Iraq
[b] Department of Physics, College of Science, University of Wasit, Kut, Iraq

Abstract

In this study, pure polyaniline (PANI) and polyaniline-based nanocomposites incorporating 5−15 % wt.% of silica@Fe_3O_4 were synthesized using ultrasonic-assisted polymerization. Formation of PANI and the well-dispersed nanocomposites was confirmed by FT-IR, UV-Vis, XRD, SEM, and TEM techniques. The XRD results showed that the particle size of pure aniline (PANI) was 55.5 nm. This size was reduced to 45.2 nm when PANI was doped with 15 % wt. of green-prepared silica@Fe_3O_4, indicating a high homogeneity and improvement in the structure of the formed nanocomposite. The optical band gap was narrowed from 3.2 to 2.5 eV with increasing of the dopant content, suggesting an enhanced charge-transfer interaction. Furthermore, a significant improvement in the electrical conductivity of the ultrasonically doped PANI was observed over the pure PANI. Additionally, it was found that that the electrical conductivity increased with increasing of doping weight ratio and increasing of temperature. These findings demonstrate that the green-synthesized silica@Fe_3O_4 effectively improves the structural and electrical properties of PANI, highlighting a new approach for producing distinct conductive nanocomposites with promising electronic applications.

Keywords: Conductivity, Green chemistry, Magnetite, Nanoparticle, Polyaniline, Silica

1. Introduction

Composites are a category of materials that significantly participate in improving human life. Composite materials are formed by joining at least two substances with distinguished characteristics [1]. Nanocomposites are class of composites distinguished by their nanometer sizes [2,3]. This class of materials has been emerged as a sufficient choice instead of micro or macro-composites that have limitation in their applications [4]. Conjugated polymers usually exhibit a slight electric conductivity. In the contrary, a high electrical conductivity is shown by the oxidized or doped polymers [5]. As a common conjugated polymer, polyaniline (PANI), however, has a distinctive electrical conductivity. This polymer also shows a significant chemical stability and can be synthesized easily. Due to the fascinating electronic and optical applications of PANI, it was attracted a lot of attention [6]. Compared to their competitors of inorganic materials, Nano-composites that originated from joining polymeric-inorganic materials exhibit an amazing performance [7]. The applications of these new classes of nano-composites present in different fields such as photodegradable properties, optical applications and developed biological electronic [8−10]. Many approaches for producing nanomaterials have been employed. These methods varied from long-route to simple green chemistry approaches [11]. A lot of attention has been paid to green chemistry techniques, principally due to the

Received 29 November 2025; revised 25 February 2026; accepted 2 March 2026.
Available online 6 April 2026

* Corresponding author.
E-mail addresses: ali@uowasit.edu.iq (A.S. Shaway), kholoud@uowasit.edu.iq (K.D. Khamkheem), jabaies@uowasit.edu.iq (J.K. Abaies), asaker@uowasit.edu.iq (A.G. Sager).

https://doi.org/10.33640/2405-609X.3456

environment-friendly besides their low coast. In this context, plant-mediated synthesis involved in green chemistry is an attractive method as they can be carried out without any reagent. Therefore, numerous metal-nanoparticles have been produced, including Au, Zn and Ag [12–14]. Nanoparticles surface can be modified via utilizing of plant extracts as they comprises different phytochemicals [15]. To synthesize electrically conductive nano-composites, the polymers with conductivity properties have been loaded by many metal and metal oxide particles. As they inherent p-type semiconductors with reasonably slight band gaps, the iron oxides display various noteworthy properties, rendering them to be used in a variety of applications [16]. Polymers have various applications in electrical and electronics manufacturing. They have been utilized as electrical or heating insulators, or as elementary substances in the electrical capacitors industry. The scope of polymers electronic applications can be expanded to involve the electrical conductivity, particular, in the synthesis of diodes and solar cells. This can be achieved through the distortion or the addition of metallic substances including Cu and Ag [17]. As a conducting polymer, the synthetic procedure of poly aniline (PANI) significantly effect on its electrical conductivity. It was stated that the electrical conductivity of polyaniline can be varied from (10-10-102) s/cm [18,19]. It is well known that aniline polymerization resulted in formation of polyaniline (PANI), which shows a high electrical conductivity. Aniline is water-soluble material due to its basicity. The weak basic feature of this substance is attributed to the lone pair electrons located on N atom in the -NH_2 moiety [20].

The aim of this research was doping of polyaniline with silica@Fe_3O_4 and studying the effect of the dopant ratio on its electrical conductivity. Doping process was conducted with nano-oxides (prepared through green chemistry methods) using an ultrasonic approach to obtain nanocomposites. Unlike conventional PANI-based nanocomposites, this study combines ultrasonic-assisted polymerization with eco-assisted synthesis of silica@Fe_3O_4 nanoparticles to enhance dispersion, interfacial interaction, and temperature-dependent electrical conductivity.

2. Materials and methods

2.1. Materials and instruments

All chemicals used in this work were of analytical grade and acquired from Sigma-Aldrich Company.

Powder X-ray diffraction (X′ Pert Pro mono achromatized) was employed to acquire the XRD patterns at the range of 5°–90°. A transmission electron microscope (TEM) [(JEM-2100 (JEOL)] was utilized to investigate the surface morphology of the synthesized polymers. An energy dispersive spectrometer (EDX) was exploited to ascertain the surface elemental constitution of polymers.

2.2. Synthesis of polyaniline

Polyaniline was synthesized by the oxidation polymerization of aniline in an acidic conditions using an ammonium persulfate as an oxidant [21]. The process begun by mixing 2.3 ml of aniline with 50 ml of HCl (0.5 M), then stirring the heterogeneous mixture until it became homogeneous solution. This was achieved by a magnetic stirring technique using a Digital Hot Plate/Stirrer device. The produced solution was left in an ice bath for about 60 min. In another container, 50 ml of distilled water was mixed with 5.7 g of ammonium persulfate. This oxidizing agent was then added to the aniline solution gradually drop by drop, where the color of the mixture was changed until it turned into dark green, indicating the completion of the polymerization process. The obtained solution was left to rest for 24 h at ambient temperature. After that, the formed precipitate was filtered and then washed with pure acetone for several times to afford a clean and a dark green solid product. This material was dried in a vacuum oven at 80 °C for 6 h before it was crushed using a mortar to obtain polyaniline powder.

2.3. Green synthesis of silica@Fe_3O_4nanoparticles

Rice husks are available as agricultural waste, so they were utilized to produce the amorphous silica. The silica was extracted from RH via the sol-gel method at pH = 6 [22], and then it was reacted with iron salts as follows: Fe_3O_4 nanoparticles were produced from silica extracted from husk. Briefly, 5 g of silica was added to 20 ml of deionized water with stirring. The synthesis of Fe_3O_4 nanoparticles was performed by mixing of 20 mL of 2 mol of $FeCl_3$ and 2 mol of $FeCl_2$ in a beaker. The produced iron chloride solution was then added to the silica solution drop by drop. To this mixture, 1 M of sodium hydroxide was added with stirring for 1.5 h until a black-colored precipitate was formed. The precipitate was obtained by filtration, washed with water for three times, and dried at ambient temperature. The resultant material was calcined at 400 °C for

2 h. The solid black-colored product was collected and kept for a further processing.

2.4. Preparation of nano-PANI/silica@Fe_3O_4 composite

Nanocomposite (PANI/silica@Fe_3O_4) was generated through the addition of (5, 10, and 15)% of the silica-iron oxide NPs to (2.5) mL of aniline. Upon the formed mixture was placed under ultrasonic waves for 15 min, hydrochloric acid (5 M, 10 mL) was added. The produced solution was slowly stirred until its color was turned into green-blackish. The solution was left to settle for one night where a precipitate was formed. The formed polymeric solid material was separated by filtration. To eliminate the short chains of the polymer, acetone was added. The obtained polymeric long-chains was dried, and gridded utilizing a Passel mortar. The produced fine powder of polyaniline (PANI) (the conducting polymer), was retained in tightly closed flask.

2.5. D.C electrical measurements

To examine the doped and pure polyaniline samples throughout the polymerization, The D.C electrical measurements were employed at several voltages. The very fine powder of the PANI was firstly subjected to a pressure of three tones to compress it in a pellet form with a 10 mm diameter and 1.68–1.98 mm thickness. The pellet surface was covered with aluminum using vapor deposition technique to expand the electrical connection. The D.C measurements were run using a series circuit technique at a temperature ranged from 303 to 423 K. Aiming to lessen stray capacitance, a special sample holder was designed and utilized for this purpose. Measurement of each pellet was repeated three times and the average value was stated. The following equation was employed to obtain the total conductivity [23]:

$$\sigma = L / (RA) \quad (1)$$

Where: L = thickness, A = cross section, R = resistance, which is calculated by Eq. (2).

$$R = V/I \quad (2)$$

V = voltage, and I = current.

To calculate the activation energy (Ea.), the following formula of Arrhenius equation was utilized [23]:

$$\sigma = A \exp(-Ea. / KB\, T) \quad (3)$$

KB = Boltzmann's constant (1.3806 × 10−23 J/K), T = Kelvin.

3. Results and discussion

Synthesis of pure polyaniline chains were conducted using ultrasonic technique in presence of HCl (as the acidic medium) at room temperature. Following the same procedure, different doped polyanilines were synthesized, but in this case different percentages of silica@Fe_3O_4 nanoparticles were added, yielding darkish green powder (Fig. 1). All reactions were carried out under oxidation environment employing ammonium persulfate (as an oxidizing agent). Scheme 1 shows the chemical oxidative polymerization.

3.1. Characterization of pure polyaniline (PANI) and doped polyaniline (S1–S3) nanocomposites

The synthesized samples were characterized using FTIR technique to identify the functional groups, XRD to analyze crystallinity, SEM and TEM to analyze the morphology, UV-Vis spectroscopy to test the optical properties, and DC electrical conductivity measurement to study of charge transport behavior.

3.1.1. FT-IR spectroscopic measurements

Fig. 2 shows FT-IR spectra of pure polyaniline (PANI) and the doped polyaniline (S1–S3) nanocomposites. The spectrum of PANI is shown in Fig. 2. The band of N–H (aromatic amine) in the benzenoid ring appears at 3419 cm^{-1} [24]. Also, the peaks observed at 3419, 1581, 1489, 1385, 1127, and 823 cm^{-1} are identical with those of the standard PANI. The bands noticed at 2924 and 2863 cm^{-1} are corresponding to alkyl groups that belong to

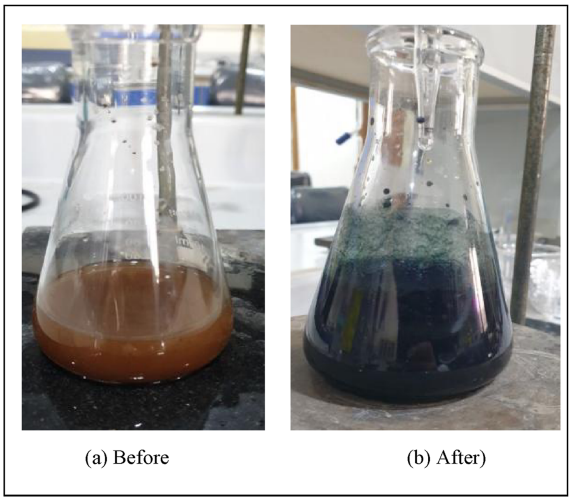

Fig. 1. The color of aniline before (a) and after (b) polymerization.

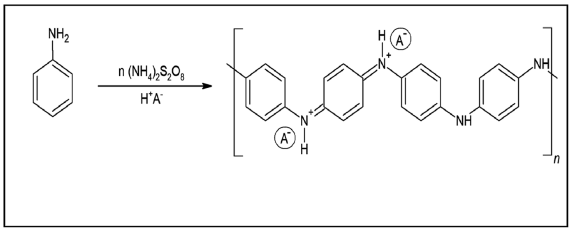

Scheme 1. Oxidative polymerization of aniline.

dodecyl hydrogen sulfate. The stretching band detected at 1631 cm^{-1} is identical with C=N of the quinoid moiety. The bands appeared at 1300-1200 cm-1 assigned to C–N in the benzenoid moieties [25]. Furthermore, some bands of the nanocomposites spectra (5–15 %) were underwent slight shifts compared to those of pure PANI (Fig. 2). These shifts due to the interaction between the Fe_3O_4@Silica nanoparticles and PANI, which probably generated between N–H groups of PANI and O–Fe and O–Si over the silica@Fe_3O_4 nanoparticles [26].

3.1.2. X-ray diffraction

Fig. 3 displays the X-ray diffraction pattern of pure polyaniline (PANI) showing its polycrystalline structure, where the peaks were detected at 2θ = (20.3, 25.1, 43.9, 64.3, 77.4) 2θ. This pattern was identical with the (JCPDS Card No. 07–0508). The PANI crystalline structure most is likely attributed to the replication of ben zenoid and quinoid moieties along the chain of PANI. The main peak observed at 2θ = 25.1 belongs to the crystal plane (110) [27–29] of polyaniline hydrochloride. The X-ray diffraction data of the PANI/SiO2@Fe3O4 (S1–S3 nanocomposites) showed a polycrystalline

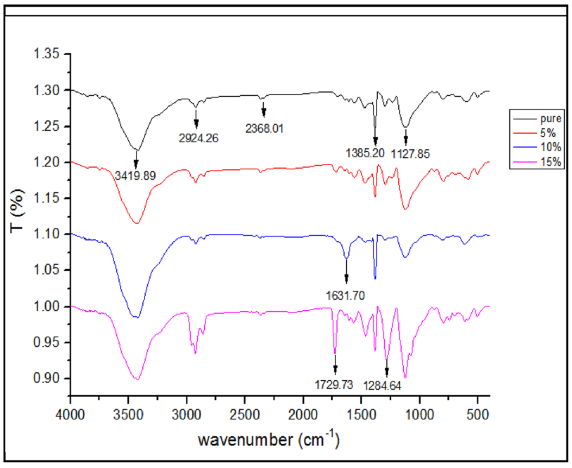

Fig. 2. FTIR spectra of PANI and silica@Fe_3O_4 nanocomposites (5–15 %).

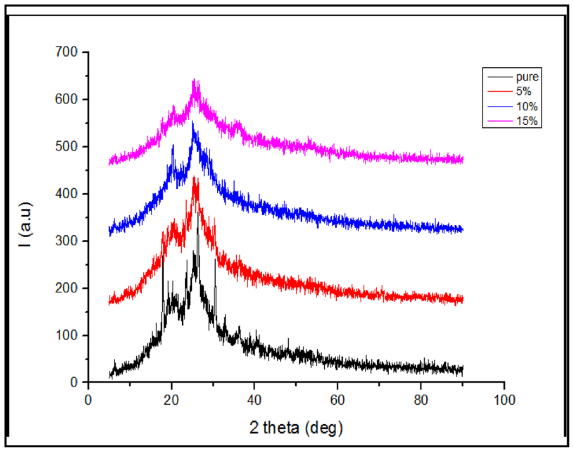

Fig. 3. X-ray diffraction of PANI-silica@Fe_3O_4 nanocomposites.

structure, but the degree of crystallization is not clear.

Hence, the intensity of the peaks decreases with increasing of doping percentage as displayed in Fig. 3. This implies that polyaniline is affected by the addition of the silica-iron oxide nanoparticles. Fig. 3 shows the polyaniline (PANI) peaks at 2θ = (43.9, 64.3, and 77.4), indicating the gradual decrease in peaks of pure polyaniline (PANI) with increasing the doping weights from 5 to 15 %wt. Nevertheless, as the silica@Fe_3O_4 nanoparticles being permeated into PANI layers, peaks of this material became very weak or mostly invisible [30].Fig. 3 also shows the results of XRD of pure and doped polyaniline powder and compared with the card (JCPDS Card No.07-0508). This figure shows that the values of the inter-crystalline plane distances that calculated by Eq. (4) are highly consistent with their values in the card as shown in (Table .1). The crystallite size (D) was also calculated by Scherer's Formula [31]:

$$n\lambda = 2d\sin(\theta) \quad (4)$$

$$k(\lambda/\beta)\cos(\theta) \quad (5)$$

Where: D = The distance between two successive atomic levels, β = The width of the curve at the midpoint of the peak in units (deg), θ = The Braak's

Table 1. Values of the inter plane distances obtained from XRD of PANI and doping PANI.

Code	2θ (Deg.)	FWHM (Deg.)	d_{hkl} Exp. (Å)	C.S (nm)
PANI pure	25.2148	0.1467	3.5291	55.5
5 % silica@Fe_3O_4	25.2485	0.1514	3.5245	53.8
10 % silica@Fe_3O_4	25.8032	0.1599	3.4500	51.0
15 % silica@Fe_3O_4	26.9354	0.1806	3.3075	45.2

angle, K= Scherer's constant (0.9) and λ = wavelength.

Scherer equation provides an estimation of average crystallite size rather than true particle size. The crystal size of the prepared compounds ranged between (55.5 and 45.2) nm, where the largest crystal size was obtained for the pure polyaniline. While the small crystal size was obtained at doping weight (15 %), which indicates a high homogeneity at this weight. The broad diffraction peak of PANI indicates its semi-crystalline property.

3.1.3. Scanning electron microscopy (SEM)

SEM images were acquired using JEOL, JSM-6330 LA at 20.0 kV and 1.0000 nA. Fig. 4(a–c) displays the surface morphology of the produced polymers. Fig. 4 (a PANI–aS3) displays the fibrous morphology of the polymer chain, which signifies the fibrous nature of the PANI layers. Fig. 4(b) shows the map images that represent the uniform distribution of silica@Fe_3O_4 nanoparticles over the PANI layers. Fig. 4(c) shows the dimensions of the particles embedded into the polymeric films with

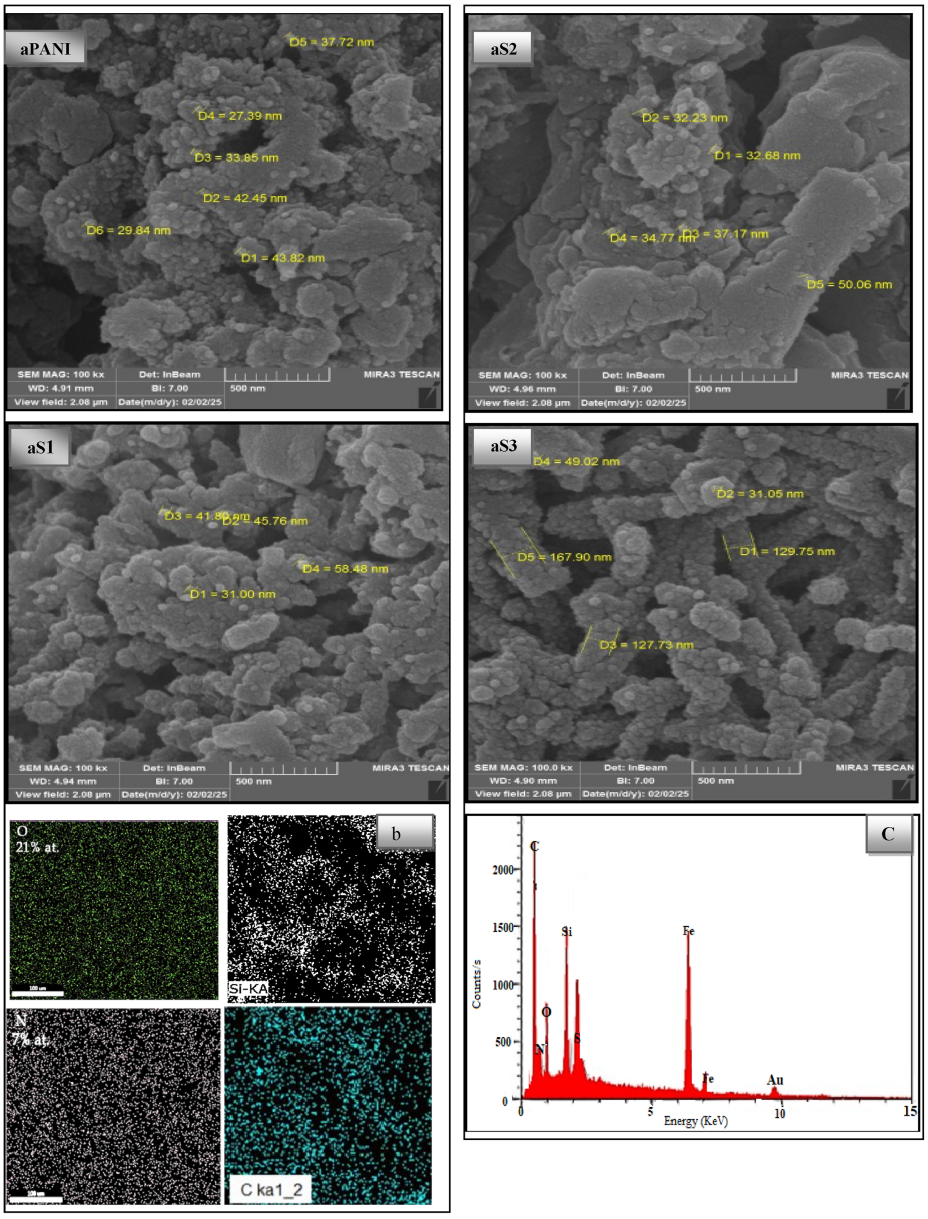

Fig. 4. FR-SEM images of polyaniline (aPANI), polyaniline (aS1) 5 %Wt, polyaniline (aS2) 10 %wt, polyaniline (aS3) 15 %wt; maps EDX of polyaniline 15 %wt (b) and EDX of the doped PANI 15 %wt (c).

range of 32–143 nm, and the homogeneous scattering of silicone, iron, sulfur, and oxygen. This clarify that these atoms were uniformly scattered around the PANI layers. Thus, the FESEM/EDX data substantiate the immobilization of iron oxide over the surface of amorphous silica, which is consistent with the XRD findings. Furthermore, the EDX data exhibited that the percentage of silicon, oxygen, and iron elements in silica@Fe_3O_4 were 38.5, 11.01 and 20.01 (wt. %), respectively. The EDX spectrum of PANI (silica@Fe_3O_4, 15 % wt.), also showed also the presence of Si and N elements.

The particle size detected by SEM represents agglomerated particles, whereas XRD reflects the crystallite size of coherent domains. SEM displays the size of aggregated particles, XRD measures crystallite size (coherent diffraction domains). Agglomeration during drying increases the apparent SEM size, and each particle may contain multiple crystallites.

3.1.4. UV-vis absorbance analysis

UV-vis absorption spectra of PANI and the produced the doped polyaniline (S1–S3 nanocomposites) are presented in Fig. 5. The absorption spectrum of pure PANI displays the characteristic bands that observed at 364 and 457 nm. The absorbance seen at 364 nm is attributed to π − π*electronic transitions occurring within the benzenoid substituents. Nevertheless, the absorption band appears at 457 nm likely belonging to polar on- π*transition, which take place due to the PANI protonation. The UV-Vis spectra of PANI nanocomposite (5–15 %) are presented in Fig. 5, which exhibits the shifting in the locations and the intensities of the distinguishing bands of PANI. These shifts are attributed to the incorporation of silica@Fe_3O_4NPs.in the polymeric net, indicating the effect doping on the PANI conductivity. The optical energy gap is the lowest energy required for transferring an electron from the valence band to the conduction band. This constant is necessary as it provides a lucid concept about optical absorption. Energy gaps are critically affected by the doping process and the environment temperature. The energy gap value of the allowed direct transition was obtained by graphically drawing the (αvh - νh) relationship. This was achieved by choosing the best tangent to the straight part of the curve to cross the energy axis of the incident photons at the point 0 = 2αvh, where the value energy gap of the allowed optical transitions signifies the point of crossing with the energy axis of the falling photon as illustrated in Fig. 6. The energy gap values for pure polyaniline and its nanocomposites ranged between (3.2–2.5) eV, and the lowest value of the energy gap was found at the (15 %) weight. The reason behind this is the presence of new local levels above the valence bands and below the conduction bands within the forbidden gap, which is compatible with previously published works [32,33]. The optical energy gap of PANI and its nanocomposites are exhibited in Table 2.

An indirect allowed transition was assumed due to the semi-crystalline polymeric nature of PANI. As baseline correction was applied to all UV-Vis spectra.

3.2. DC-electrical conductivity

One of the aims of the present study was to investigate the effect of doping ratios on the electrical properties of polyaniline. Fig. 7 shows the role

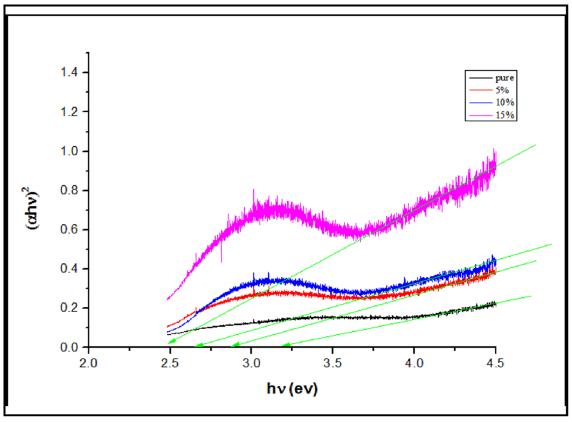

Fig. 5. Absorbance spectrum (UV-Visible) of pure and doped polyaniline (5–15 %Wt).

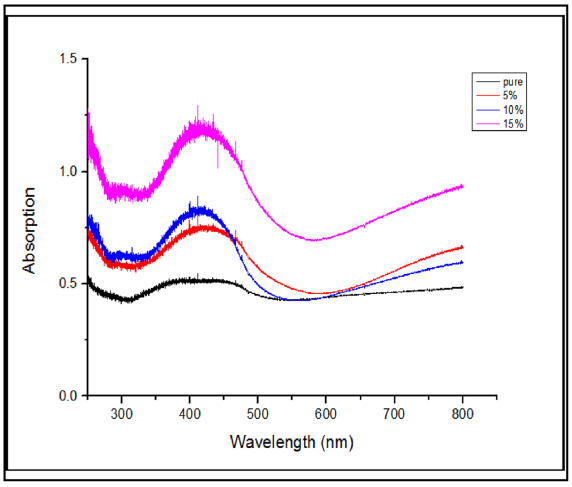

Fig. 6. Optical energy gap of polyaniline and nanocomposites.

Table 2. The optical energy gap of pure polyaniline and its nanocomposites.

Sample	PANI	5 %	10 %	15 %
E_g(ev)	3.2	2.9	2.7	2.5

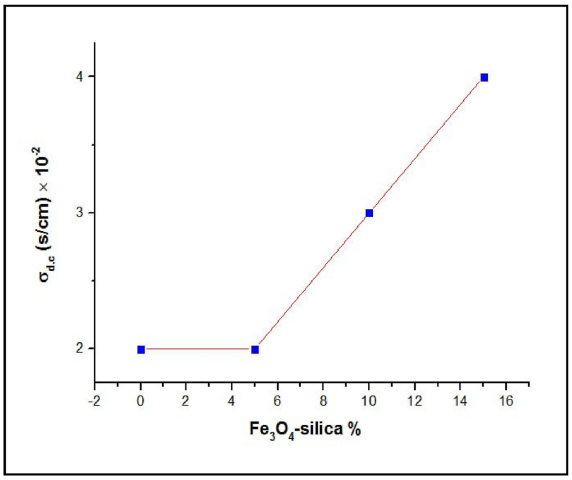

Fig. 7. Effect of doping ratio on polyaniline conductivity at 20 °C.

of doping ratios of silica@Fe_3O_4 nanoparticles on the electrical conductivity values of the nano-composite at a temperature of 20C°. It was observed from the figure that increased with the increasing of doping weight percentage. Compared to other percentages doping weight, the highest value of electrical conductivity was found at the doping weight of (15 %) then 10 % shown in Table 3.

These results were compatible with the results of XRD measurements, where the slightest crystal size was found at doping weight of (15 %), indicating a high homogeneity at this weight. Also, the electro conductivity of the doped polyaniline (S3), which is consistent with the lowest value of the energy gap was observed at the doping weight of (15 %). It can be noticed that after nano-silica (SiO_2) and nano-particles of iron oxide (Fe_3O_4 or Fe_2O_3) are being incorporated into polyaniline (PANI) chains, its energy band gap was reduced. This can be assigned to a number of reasons. First, the attendance of formed nanoparticles can enhance the polymer chains assembly, which enable the extending of π-π conjugation. This allows the electrons delocalization along the polymer chain, enabling an efficient decrease in the HOMO − LUMO energy gab. The second reason is the interaction of the functional groups on the surface of nanoparticles with the nitrogen-including groups in the PANI backbone, which lead to new states of decentralized energy in the band structure. Consequently, the effective band gap will be minimized. Also, the nanoparticles features such as the semi-conductive or conductive contribute in improving charge transfer and decreases the energy levels for electronic transitions. These characteristics synergistically lead to enhancement of electrical conductivity and an apparent reduction in the optical band gap of the prepared nanocomposite [34].

Fig. 8 shows effect of doping ratio on polyaniline conductivity at 170 °C.

Table 3. Electrical conductivity of pure and doped polyaniline at temperature (20 °C).

Code	$_{dc}$(20 °C) (s/cm) σ	$_{dc}$(170 °C) (s/cm) σ
PANI(Pure)without ultrasounic	4×10^{-4}	7×10^{-4}
PANI(Pure) with ultrasounic	2×10^{-2}	4×10^{-2}
Fe_3O_4@silica 5 %wt (S1)	2×10^{-2}	6×10^{-2}
Fe_3O_4@silica 10 %wt (S2)	3×10^{-2}	1×10^{-2}
Fe_3O_4@silica 15 %wt (S3)	4×10^{-2}	3×10^{-2}

4. Conclusion

In this work, polyaniline/silica@Fe_3O_4 nanocomposites and doped polyaniline were successfully synthesized. Structural and morphological analysis confirmed the effective incorporation of silica@Fe_3O_4NPs into the PANI matrix and the improvement in particle dispersion due to ultrasonic irradiation. XRD results indicated the semi-crystalline nature of PANI and revealed changes in crystallite size and peak intensity upon nanoparticle loading, reflecting enhanced interfacial interactions within the nanocomposites. Optical studies demonstrated a slight modification in optical band gap with increasing silica@Fe_3O_4NPs, which is attributed to changes in electronic structure and localized states induced by the fillers.

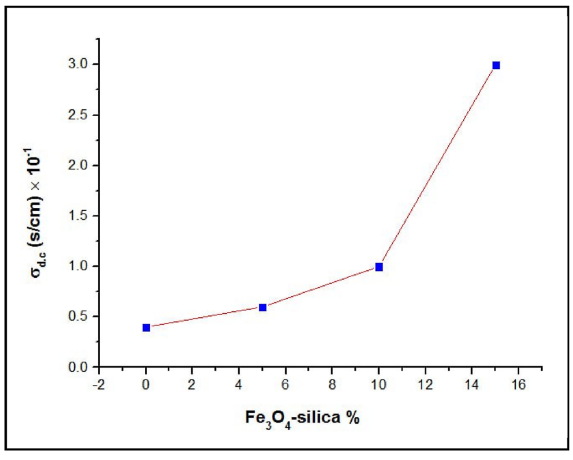

Fig. 8. Effect of doping ratio on polyaniline conductivity at 170 °C.

While electrical conductivity increases with increasing temperature, confirming the semiconducting behavior is mainly governed by thermally activated charge transport and hopping conduction mechanisms. The incorporation of silica@Fe_3O_4NPs led to a noticeable enhancement in electrical conductivity compared to pure PANI, owing to improved charge carrier mobility and better interfacial connectivity. Overall, the ultrasonic-assisted, eco-assisted synthesis route proved to be an effective method for preparing PANI/silica@Fe_3O_4 nanocomposites with improved structural uniformity and electrical performance. These polymers show potential for applications in temperature-dependent electronic devices, sensors, and conductive polymer-based systems.

Ethics information

This study does not involve human participants or animals. Therefore, ethical approval was not required.

Funding statement

This research received no specific grant from any funding agency in the public, private, or not-for-profit sectors.

Conflicts of interest

The authors declare that they have no competing interests.

Acknowledgment

The authors would like to thank the College of Science, University of Wasit, for providing the necessary facilities.

Supplementary material

https://kijoms.uokerbala.edu.iq/cgi/editor.cgi?article=3456&window=additional_files&context=home.

References

[1] G.T. Tran, T.T. Nguyen, T.V. Tran, Synthesis strategies, functionalization, and biomedical applications of MOF/MXene hybrid composites, Coord. Chem. Rev. 544 (2025) 217002, https://doi.org/10.1016/j.ccr.2025.217002.
[2] S. Hasan, M.F. Ibtahsum, Composite materials:fundamentals applications, Mater. Today Proc. 45 (2021) 123–129, https://doi.org/10.1016/j.matpr.2021.01.015.
[3] T. Hassan, A.K. Srivastwa, S. Sarkar, G. Majumdar, Characterization of plastics and polymers: a comprehensive study, IOP Conf. Ser. Mater. Sci. Eng. 1225 (2022) 012033, https://doi.org/10.1088/1757-899X/1225/1/012033.
[4] H. Zhang, Y. Chen, J. Wang, Green synthesis of Fe_3O_4 @SiO_2 core–shell nanostructures and their application in polymer nanocomposites, J. Mater. Sci. 57 (2022) 14520–14534, https://doi.org/10.1016/j.jallcom.2023.169639.
[5] A.G. MacDiarmid, Polyaniline: a novel conducting polymer, Synth. Met. 84 (1997) 27–34, https://doi.org/10.1016/S0379-6779(96)80112-3.
[6] S. Zhang, L. Mingjun, B. Zeng, H. Duan, D.Z. Mengqiu, Study on the electronic structures and transport properties of the poly porphyrin nanoribbons with different edge configurations, Phys. Lett. A. 382 (2018) 2769–2775, https://doi.org/10.1016/j.physleta.2018.07.046.
[7] S. Yuan, J. Hu, J. Yang, Fabrication of novel thermoplastic polyurethane elastomers with both heat resistance and conductivity prepared from p-phenylene diisocyanate, J. Appl. Polym. Sci. 142 (2025) 9047554, https://doi.org/10.1155/2022/9047554.
[8] A.H. Majeed, L.A. Mohammed, O.G. Hammoodi, S. Sehgal, M.A. Alheety, K.K. Saxena, S.A. Dadoosh, I.K. Mohammed, M.M. Jasim, N.U. Salmaan, A review on polyaniline: synthesis, properties, nanocomposites, and electrochemical applications, Int. J. Polym. Sci. 1 (2022) 9047554, https://doi.org/10.1155/2022/9047554.
[9] C.V. Kattookaran, R. Govindasamy, S.P. Selvam, D. Viswanathan, Biosynthesis of Ag doped MgO-ZnO nanocomposite with cassia Alata plant leaves extract and assessment of their biological applications, Next Mater. 8 (2025) 100820, https://doi.org/10.1016/j.nxmate.2025.100820.
[10] A. Garima, D. Sharma, N. Mittal, Greener nano materials for soft tissue regeneration: diagnostic and therapeutic advances, J. Drug Deliv. Sci. Technol. 106 (2025) 106747, https://doi.org/10.1016/j.jddst.2025.106747.
[11] R.A. Jesus, G.C. de Assis, R.J. de Oliveira, J.A.S. Costa, C.M.P. Silva, H.M.N. Iqbal, L.F.R. Ferreira, Metal/metal oxide nanoparticles: a revolution in the biosynthesis and medical applications, Nano-Struct. Nano-Objects 37 (2024) 101071, https://doi.org/10.1016/j.nanoso.2023.101071.
[12] L.M.S. Brandão, M.S. Barbosa, R.A. Jesus, P.A. Bharad, Á.S. Lima, C.M.F. Soares, R.M.N. Yerga, M. Bilal, L.F.R. Ferreira, H.M.N. Iqbal, C.S. Gopinath, R.T. Figueiredo, Enhanced hydrogen fuel production using synergistic combination of solar radiation and TiO_2 photocatalyst coupled with burkholderia cepacia lipase, Int. J. Hydrogen Energy 47 (2022) 14483–14492, https://doi.org/10.1016/j.ijhydene.2022.02.220.
[13] L. Zuo, A. Wang, Green synthesis of CuONPs through phytochemical reduction of matricaria Chamomilla leaves extract and their antifungal potential against fusarium wilt in tomato plants, S. Afr. J. Bot. 185 (2025) 53–65, https://doi.org/10.1016/j.sajb.2025.07.048.
[14] P.S.A. Gautam, A.K. Singh, R.S. Singh, Recent advances in rare earth doped metal oxide based nanomaterials for supercapacitors, J. Energy Storage. 131 (2025) 117431, https://doi.org/10.1016/j.est.2025.117431.
[15] C. Zhang, Y. Zheng, J. Jing, Y. Liu, H. Huang, A comparative study on aluminum electrolytic capacitors: from liquid state electrolyte, solid-state polymer to their hybrid, J. Clean. Prod. 375 (2022) 134044, https://doi.org/10.1016/j.jclepro.2022.134044.
[16] M.R.Y.M. Cord, A. Seppälä, M. Pourakbari, J.B. Kasmaei, O.J.Z. Rojas, From low conductivity to high energy efficiency: the role of conductive polymers in phase change materials, Chem. Eng. J. 508 (2025) 160804, https://doi.org/10.1016/j.cej.2025.160804.
[17] Z. Yu, Z. Yu, L. Chen, Y. Yan, M. Yao, J. Chen, S. Zhao, H. Xu, F. Wang, W. Teng, Z. Ye, X. Jin, A novel visual simulation assisted vacuum-impregnation strategy for titanium nanotube-based antibacterial coating preparation and application, Chem. Eng. J. 508 (2025) 160785, https://doi.org/10.1016/j.cej.2025.160785.

[18] X. Wu, Y. Zhou, J. Yang, X. Liang, Y. Xin, Q. Yang, G. Chen, C. Zeng, X. Lan, W. Zhao, Y. Liu, Electrically conductive functionalization of cured polyether ether ketone with improved bioactivity by surface-polymerization of polyaniline, Chem. Eng. J. 499 (2024) 156169, https://doi.org/10.1016/j.cej.2024.156169.
[19] A.J. Ležaić, D.B. Bogdanović, G.Ć. Marjanović, In sit Raman spectroscopy study of the oxidative polymerization of aniline in media of different acidity, Synth. Met. 305 (2024) 117602, https://doi.org/10.1016/j.synthmet.2024.117602.
[20] M. Beygisangchin, S. Abdul Rashid, S. Shafie, A.R. Sadrolhosseini, H.N. Lim, Preparations, properties, and applications of polyaniline and polyaniline thin films-a review, Polym 13 (2021) 2003, https://doi.org/10.3390/polym13122003.
[21] J.A.G. MacDiarmid, A.J. Epstein, The concept of secondary doping in PANI and its impact on conductivity, Synth. Met. 69 (1995) 85–92, https://doi.org/10.1016/0379-6779(94)90171-6.
[22] K.M. Hello, A.-T. Mohammad, A.G. Sager, Solid urea sulfate catalyst for hydrolysis of cellulose, Waste Biomass Valor. 8 (2017) 2621–2630, https://doi.org/10.1007/s12649-016-9693-z.
[23] P. Li, J. Li, F. Liu, Jiannan, J. Shi, K. Yu, H. Xu, F. Su, K. Wang, S. Li, Y. Zhang, Ternay nano hybrids of MIL-125 derivatives(C-TiO_2) and nano-Pd dual-hybridized polyaniline (PANI) for enhanced NH_3 gas sensing performance, Chem. Eng. J. 515 (2025) 163425, https://doi.org/10.1016/j.cej.2025.163425.
[24] T. AlZoubi, M. Al-Gharram, G. Makhadmeh, O. Abu Noqta, Comparative analysis of optoelectronic and structural characteristics in electrochemically synthesized hybrid -nanocomposites based on PANI-CSA/metal oxide nanoparticles, Phys. B: Condens. Matter. 713 (2025) 417380, https://doi.org/10.1016/j.physb.2025.417380.
[25] A.S. Shawai, A.F. Essa, Preparation and study of the structural and optical properties for polyaniline/Cu nanocomposite, Mater. Today Proc. 45 (2021) 5804–5808, https://doi.org/10.1016/j.matpr.2021.03.171.
[26] H.N. Sumedha, M. Shashank, B.M. Praveen, G. Nagaraju, Electrochemical activity of ultrathin MoO_3 nano flakes for long cycle lithium ion batteries, Res. Chem. 4 (2022) 100493, https://doi.org/10.1016/j.rechem.2022.100493.
[27] X. Lu, F. Luo, W. Zhang, Q. Tian, Z. Sui, J. Chen, Enhancing the performance of manga nous oxide nanoparticles for lithium storage by in-situ construction of porous carbon embedment, Appl. Surf. Sci. 552 (2021) 149531, https://doi.org/10.1016/j.apsusc.2021.149531.
[28] D. Parajuli, S. Uppugalla, N. Murali, A. Ramakrishna, B. Suryanarayana, K. Samatha, Synthesis and characterization MXene-ferrite nanocomposites and its application for dying and shielding, Inorg. Chem. Commun. 148 (2023) 110319, https://doi.org/10.1016/j.inoche.2022.110319.
[29] N. Rani, S. Chahal, A.S. Chauhan, P. Kumar, R. Shukla, S.K. Singh, X-ray analysis of MgO nanoparticles by mod ified Scherer's Williamson-hall and size-strain method, Mater. Today Proc. 12 (2019) 543–548, https://doi.org/10.1016/j.matpr.2019.03.096.
[30] I.S. Elashmawi, H.M. Alhusaiki-Alghamdi, Fabrication, characterization, spectroscopic, and magnetic properties of polyaniline/magnetite (PANI/Fe_3O_4) nanocomposites, Opt. Quant. Electron. 56 (2024) 1090, https://doi.org/10.1007/s11082-024-06843-4.
[31] S. Rafiq, M.A. Lovely, S.R. Mim, M.S. Islam, M. Hasan, M.M. Billah, Structure controlled enhanced photocatalytic activity of polyaniline (PANI)-ZnO nanocomposites, Heliyon 11 (2025) e42888, https://doi.org/10.1016/j.heliyon.2025.e42888.
[32] A. Khalid, R.M. Ahmed, M. Taha, T.S. Soliman, Fe_3O_4 nanoparticles and Fe_3O_4@SiO_2 core-shell: synthesize, structural, morphological, linear, and nonlinear optical properties, J. Alloys Compd. 934 (2023) 169639, https://doi.org/10.1016/j.jallcom.2023.169639.
[33] J.A. Oyetade, R.L. Machunda, A. Hilonga, Functional impacts of polyaniline in composite matrix of photo catalysts: an instrumental overview, RSC Adv. 13 (2023) 15467–15489, https://doi.org/10.1039/D3RA01243C.
[34] I. Sapurina, J. Stejskal, The mechanism of the oxidative polymerization of aniline and the formation of supramolecular polyaniline structures, Polym. Int. 57 (2008) 1295–13251, https://doi.org/10.1002/pi.2476.